Stability-Oriented Minimum Switching/Sampling Frequency for Cyber-Physical Systems

Grid-Connected Inverters Under Weak Grid

Wang, Rui; Sun, Qiuye; Zhang, Huaguang; Liu, Lei; Gui, Yonghao; Wang, Peng

Published in:
I E E E Transactions on Circuits and Systems Part 1: Regular Papers

DOI (link to publication from Publisher):
10.1109/TCSI.2021.3113772

Publication date:
2022

Document Version
Accepted author manuscript, peer reviewed version

Stability-Oriented Minimum Switching/Sampling Frequency for Cyber-Physical Systems: Grid-Connected Inverters Under Weak Grid

Rui Wang, *Student Member, IEEE*, Qiuye Sun, *Senior Member, IEEE*, Huaguang Zhang, *Fellow, IEEE*, Lei Liu, *Senior Member, IEEE*, Yonghao Gui, *Senior Member, IEEE*, and Peng Wang

***Abstract*— Although the cyber-physical system stability is widely studied, scholars focus more on system stability with communication time delay. Therein, grid-connected inverters with the digital control system are regarded as one simplest and typical cyber-physical system. Meanwhile, the switching/sampling frequency of the inverter is always selected as low as possible from an efficiency viewpoint, resulting in unavoidable delay time. This delay time is apt to cause the system instability, which is more prone to severity under weak grid. To this end, this paper provides a minimum switching/sampling frequency for grid-connected inverters. Firstly, the system impedance model with equivalent delay time is constructed, which is based on padé approximate approach. This equivalent delay time consists of three parts, i.e., sampling delay time in cyber/physical level, calculation delay time in cyber level and pulsewidth modulation delay time in physical level, which reflects the cyber-physical interaction impact. Furthermore, the stability forbidden criterion is applied to make the switching/sampling frequency solving process become Hurwitz matrix identification problem through space mappings. Based on these space mappings, an adaptive step search approach is adopted to obtain the minimum switching/sampling frequency. Finally, the proposed approach can well evaluate the system stability under different frequencies through simulation and experiment.**

***Index Terms*— Cyber-physical system, grid-connected inverter, minimum switching/sampling frequency, adaptive step search approach.**

Manuscript received July 27, 2021; revised September 7, 2021; accepted September 16, 2021. This work was supported by the National Key Research and Development Program of China under Grant 2018YFA0702200. This article was recommended by Associate Editor Y. Tang. *(Corresponding author: Qiuye Sun.)*

Rui Wang, Qiuye Sun, and Huaguang Zhang are with the College of Information Science and Engineering, Northeastern University, Shenyang, Liaoning 110819, China (e-mail: 1610232@stu.neu.edu.cn; sunqiuye@ise.neu.edu.cn; zhanghuaguang@ise.neu.edu.cn).

Lei Liu is with the College of Science, Liaoning University of Technology, Jinzhou, Liaoning 121001, China (e-mail: liulei@lnut.edu.cn).

Yonghao Gui is with the Department of Electronic Systems, Automation and Control Section, Aalborg University, 9220 Aalborg, Denmark (e-mail: yg@es.aau.dk).

Peng Wang is with the School of Electrical and Electronic Engineering, Nanyang Technological University, Singapore 639798 (e-mail: epwang@ntu.edu.sg).

Color versions of one or more figures in this article are available at https://doi.org/10.1109/TCSI.2021.3113772.

Digital Object Identifier 10.1109/TCSI.2021.3113772

I. Introduction

RECENTLY, with the rapid development regarding information technology consisting of internet approach, communication approach, cloud computing approach and so on, cyber-physical systems (CPSs) have been introduced in detail through National Science Foundation in USA [1]. CPS has become one close coupling and collaboration between computing resources and physical resources, which makes the system more adaptive, autonomous, reliable, and available [2]. Although the cyber-physical system stability has been widely studied, almost scholars focus more on system stability with communication time delay or attack [3]-[4]. However, the stability analysis of cyber-physical systems without communication network is still blank. Furthermore, grid-connected inverters with the digital control system can be regarded as one simplest and typical cyber-physical system. Meanwhile, the switching/sampling frequency of the inverter is always selected as low as possible from an efficiency viewpoint, resulting in unavoidable delay time [5]. Furthermore, in 2020, the power-information hybrid signal delivery strategy is proposed in Nature Communications [6]. This method does not need the traditional communication network, but transmits signal through the two degrees of freedom regarding switching frequency and phase deviation of PWM in the physical layer. This method combines the cyber system and physical system into one whole. In order to ensure that each agent demodulation window does not interfere with each other, this method needs a series of orthogonal switching frequencies to transmit information. With the decrease of switching frequency, it will also lead to the problem of low-frequency/sub-synchronous oscillation. The method of this paper mainly studies the cyber-physical stability in these two cases, and provides the stability-oriented minimum switching frequency of IGBT in the inverter.

Traditionally, the system stability of cyber-physical systems was widely studied, which could be divided into two parts, i.e., stability analysis with network attack and stability analysis without network attack [7-11]. From the viewpoint of stability analysis with network attack, the current researches have constructed one relatively complete research system from the perspectives of network attack [7], attack cascade reaction [8],

network attack defense [9]. From the viewpoint of stability analysis without network attack, the current researches focused on the time delay regarding distributed/centralized communication network [10-11]. The literatures [10] and [11] respectively designed delay time threshold conditions for communication delay time caused by cyber-physical material integration in cyber-power system and cyber-energy system. Since the power system with digital control system is one simplest cyber-physical system, the stability of this control system without communication network should be studied, which belongs to small-signal stability analysis.

In the past, the small-signal stability analysis approach regarding microgrids with numerous inverters could be divided into two types, i.e., state-space function approach and impedance approach [12]-[13]. For the state-space function approach, the partial state-space function without inner current-voltage controller was established to analyze the system stability in [14]. Additionally, the overall state-space function with inner current-voltage controller was built in [15]. For complex microgrid with high order information, the model reduced order approach was proposed in [16]. However, it was difficult for scholars to build the whole state-space function regarding the microgrid with thousands of inverters [17]. Based on this, the impedance approach was proposed for the complex microgrid in recent years [18]. The impedance approach was applied to power system in 1976 through Middlebrook and J. M. Undrill [19]-[20]. Furthermore, the impedance approach was applied for DC microgrids and AC microgrids through Nyquist curve (NC) or generalized Nyquist curve (GNC) [21]. However, the restriction of the GNC was that, due to the complex matrix product formation, it was not acceptable for system design [22]. Based on this, the simplified stability criteria were proposed in turn to provide stability analysis approach without GNC drawing process, which can be divided into two types, i.e., norm-based stability criteria and stability forbidden region criteria [22]-[24]. Nevertheless, the foresaid simplified stability criteria have one main problem, e.g., high conservatism. The high conservatism (also named high conservative) is the term for control field, which is an important index of stability criteria. Therein, the high conservatism represents low accuracy of stability criteria, and the low conservatism represents high accuracy of stability criteria [21]. Meanwhile, these stability criteria paid more attention on stability operation point identification or return-ratio matrix stability margin, and it was not suitable for the switching/sampling frequency threshold value identification regarding grid-connected inverters with the digital control system, which is called high inapplicability.

In order to solve these two issues, i.e., high conservatism and high inapplicability, this paper proposes an adaptive step search approach with low conservatism to obtain the minimum switching/sampling frequency. The main advantages can be described as follows:

(*i*) In order to reflect the cyber-physical interaction impact regarding grid-connected inverters with the digital control system, the equivalent delay time consisting of sampling delay time in cyber/physical level, calculation delay time in cyber level and pulsewidth modulation delay time in physical level, is constructed through the system impedance model. Based on this, the cyber-physical interaction impact problem can be transformed into the switching/sampling frequency threshold identification problem, which is an indispensable preprocess.

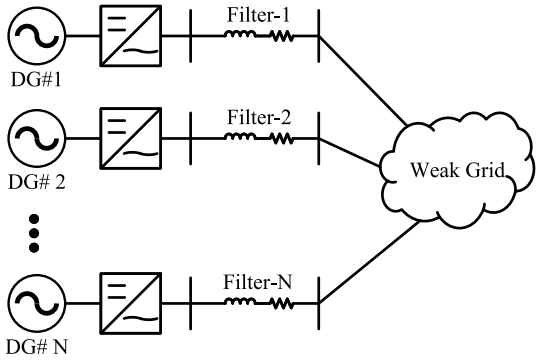

Fig. 1. Grid connected inverter with digital control system.

(*ii*) Based on the novel stability forbidden region criterion with low conservatism proposed in our previous literature [19], the switching/sampling frequency threshold identification regarding grid-connected inverters with the digital control system is switched into the identification problem whether the generalized return-ratio matrix is one Hurwitz matrix. With these effects, thousands of Nyquist curve drawing process can be eliminated, which reduces the computational burden.

(*iii*) In order to obtain the switching/sampling frequency threshold value regarding grid-connected inverters with the digital control system, an adaptive step search approach with low conservatism is proposed. Meanwhile, the convergence of the proposed adaptive step search approach is verified, and this approach is independent for the initial condition, which illustrates the high applicability of the proposed approach.

II. Generalized Return-Ratio Matrix Modeling

Traditionally, grid-connected inverters with the digital control system are shown in Fig. 1. Compared with the grid-connected inverter with $P\&Q$ controller, the grid-connected inverter with droop controller has better system stability [25]. Based on this, the grid-connected inverter with droop controller has been widely applied into weak grid to improve system stability. Therein, the detailed control strategy regarding droop controller can be found in the literature [25], which is shown in Fig. 2. Noting that the system is likely to be unstable in the case of weak grid [21]. From the viewpoint of the stability assessment, the short circuit ratio (SCR) has been widely applied in the existing researches. According to IEEE standard, the grid is considered weak for SCR below 6 to 10.

A. Time Delay Analysis

Grid-connected inverters with the digital control system are regarded as one simplest and typical cyber-physical system. Meanwhile, the switching/sampling frequency of the inverter is always selected as low as possible from an efficiency viewpoint, resulting in unavoidable delay time. In this decentralized

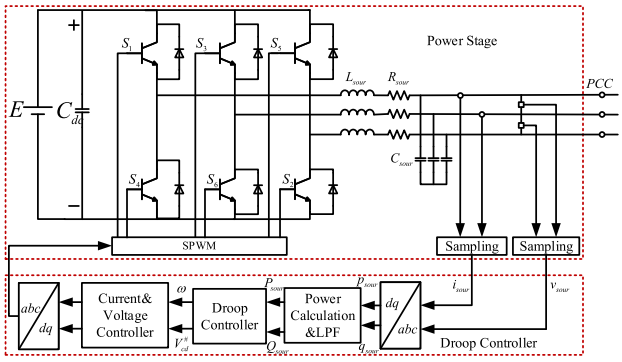

Fig. 2. Control structure of the grid connected inverter.

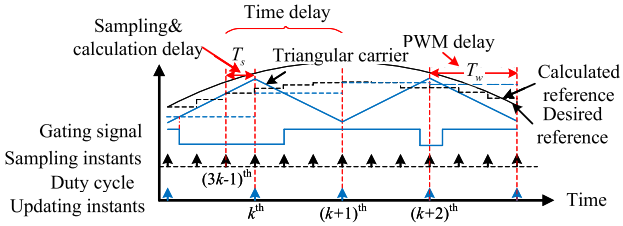

Fig. 3. Time-delay components.

control, the cyber-physical system exists unavoidable delay time including sampling delay time in cyber/physical level, calculation delay time in cyber level and pulsewidth modulation delay time in physical level, which reflects the cyber-physical interaction impact. In this paper, this equivalent delay time is defined as $G(\tau)$. Noting that this time delay arises from real-world applications, which is inversely proportional to the switching frequency [26]. As shown in Fig. 3, the equivalent delay time regarding grid-connected inverters with the digital control system can be divided into two part, i.e., the equivalent delay time regarding sampling & calculation delay time ($G(\tau_1)$) and pulsewidth modulation delay time ($G(\tau_2)$). Therein, $\tau_1 = T_s$, and T_s represents sampling period, which is the inverse of the sampling frequency $T_s = 1/f_s$. Meanwhile, $\tau_2 = 0.5T_w$, and T_w represents pulsewidth modulation period, which is the inverse of the pulsewidth modulation frequency $T_w = 1/f_w$. Traditionally, the sampling period and pulsewidth modulation period are always set as the same value [26]. Based on this, the equivalent delay time regarding grid-connected inverters with the digital control system can be represented as $G(\tau) = e^{-\tau s} = e^{-1.5T_s s} = e^{-1.5T_w s} = e^{-1.5Ts}$, where T represents system sampling period or pulsewidth modulation period (called switching period). Noting that the researches regarding the traditional time delay is indeed a common topic, which mostly refers to the time delay caused through communication networks. The research in this paper is one nanosecond or microsecond time delay, which is consisting of sampling delay time in cyber/physical level, calculation delay time in cyber level and pulsewidth modulation delay time in physical level. This time delay reflects the cyber-physical interaction impact.

B. System Modeling

According to the impedance-based approach, the overall system can be divided into two subsystems under $d-q$ axis,

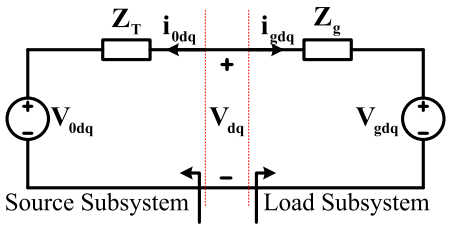

Fig. 4. Thevenin equivalent circuit of interconnected system.

i.e., source subsystem and load subsystem, which is shown in Fig. 4. Therein, the source subsystem output impedance matrix and load subsystem input admittance matrix can be obtained as follows: The dynamic characteristics of voltage and current of the droop controller under $d-q$ axis are shown below [5]:

$$V_{sourd} = I_{sourd}(R_{sour} + sL_{sour}) - \omega L_{sour} I_{sourq} + V_{cd}, \quad (1)$$

$$V_{sourq} = I_{sourq}(R_{sour} + sL_{sour}) + \omega L_{sour} I_{sourd} + V_{cq}, \quad (2)$$

$$I_{sourd} = C_{sour} V_{cd} s - \omega C_{sour} V_{cq} + I_{cd}, \quad (3)$$

$$I_{sourq} = C_{sour} V_{cq} s + \omega C_{sour} V_{cd} + I_{cq}, \quad (4)$$

where V_{sourd}, V_{sourq}, I_{sourd} and I_{sourq} represents the output voltage and output current of the grid-connected inverter under $d-q$ axis, respectively. V_{cd}, V_{cq}, I_{cd} and I_{cq} represents the voltage and current of the grid-connected inverter under $d-q$ axis, respectively. R_{sour}, L_{sour} and C_{sour} represents the resistor, inductor and capacitor of the RLC filter, respectively. Furthermore, the cascaded voltage/current double loop controller is shown as follows:

$$I^{\#}_{sourd} = G_v^{sour}(V^{\#}_{cd} - V_{cd}) - \omega C_{sour} V_{cq} + K I_{cd}, \quad (5)$$

$$I^{\#}_{sourq} = G_v^{sour}(V^{\#}_{cq} - V_{cq}) + \omega C_{sour} V_{cd} + K I_{cq}, \quad (6)$$

$$V^{\#}_{sourd} = G_i^{sour}(I^{\#}_{cd} - I_{cd}) - \omega L_{sour} I_{cq} + V_{cd}, \quad (7)$$

$$V^{\#}_{invq} = G_i^{inv}(I^{\#}_{cq} - I_{cq}) + \omega L_{inv} I_{cd} + V_{cq}, \quad (8)$$

where $I^{\#}_{cd}$, $I^{\#}_{cq}$, $V^{\#}_{cd}$ and $V^{\#}_{cq}$ represents voltage and current signal of the grid-connected inverter under $d-q$ axis, respectively. G_v^{sour} and G_i^{sour} represents the cascaded voltage/current double loop controller ($G_v^{sour} = k_{vp}^{sour} + k_{vi}^{sour}/s$ and $G_i^{sour} = k_{ip}^{sour} + k_{ii}^{sour}/s$). K represents feedback factor. Additionally, the instantaneous active power p_{sour} and reactive power q_{sour} are provided through equations (9)-(10). The low-pass filter is applied to the grid-connected inverter to obtain the average active power P_{sour} and reactive power Q_{sour}. Based on this, the output active power and reactive power of the grid-connected inverter are expressed as follows:

$$p_{\text{sour}} = 1.5\left(V_{cd} I_{cd} + V_{cq} I_{cq}\right), \quad (9)$$

$$q_{\text{sour}} = 1.5\left(V_{cd} I_{cq} - V_{cq} I_{cd}\right), \quad (10)$$

$$P_{sour} = \frac{\omega_c}{s + \omega_c} p_{sour}, \quad (11)$$

$$Q_{sour} = \frac{\omega_c}{s + \omega_c} q_{inv}, \quad (12)$$

where ω_c represents the cut-off frequency regarding low-pass filter. Considering the equivalent delay time impact, the

equations (11)-(12) can be rewritten as follows:

$$P_{sour} = \frac{\omega_c}{s+\omega_c} e^{-1.5Ts} p_{sour}, \tag{13}$$

$$Q_{sour} = \frac{\omega_c}{s+\omega_c} e^{-1.5Ts} q_{sour}, \tag{14}$$

where s represents the Laplace factor. Noting that $e^{-\tau s} \approx \sum_{k=0}^{n} (-1)^k c_k \tau^k s^k / \sum_{k=0}^{n} c_k \tau^k s^k$, where $c_k = [(2n-k)!n!]/[2n!k!(n-k)!]$. According to the literature [10], the foresaid section can be simplified as $e^{-1.5Ts} = 4f-3s/4f+3s$, where f represents the system sampling or switching frequency. The droop controller can be expressed as:

$$\omega = \omega^{\#} - mP_{sour}, \tag{15}$$

$$V_{cd}^{\#} = V^{\#} - nQ_{sour}, \tag{16}$$

where $\omega^{\#}$ and $V^{\#}$ represents rated angular speed and voltage, respectively. According to the dynamic phase approach [21], the small-signal analysis regarding the equations (1)-(2) and (7)-(8). Therein, the main principles used are $x = y = x^{\#} + \Delta x = y^{\#} + \Delta y \rightarrow \Delta x = \Delta y$. the small-signal model regarding $\Delta I_{sour}^{\#}$ can be shown as follows:

$$\begin{bmatrix} \Delta I_{sourd}^{\#} \\ \Delta I_{sourq}^{\#} \end{bmatrix} = [B1]_{2*2} \begin{bmatrix} \Delta I_{sourd} \\ \Delta I_{sourq} \end{bmatrix} + [B2]_{2*2} \begin{bmatrix} \Delta\omega \\ \Delta V_{cd}^{\#} \end{bmatrix}, \tag{17}$$

where

$$[B1]_{2*2} = \begin{bmatrix} \frac{R_{sour}+sL_{sour}+G_i^{sour}(s)}{G_i^{sour}(s)} & 0 \\ 0 & \frac{R_{sour}+sL_{sour}+G_i^{sour}(s)}{G_i^{sour}(s)} \end{bmatrix}$$

and $[B2]_{2*2} = \begin{bmatrix} -\frac{I_{sourq}^{\#} L_{sour}}{G_i^{sour}(s)} & 0 \\ \frac{I_{sourd}^{\#} L_{sour}}{G_i^{sour}(s)} & 0 \end{bmatrix}$.

Furthermore, the small-signal model regarding the equations (3)-(6) can be shown as follows:

$$\begin{bmatrix} \Delta I_{sourd} \\ \Delta I_{sourq} \end{bmatrix} = \begin{bmatrix} \Delta I_{cd} \\ \Delta I_{cq} \end{bmatrix} + [B3]_{2*2} \begin{bmatrix} \Delta V_{cd} \\ \Delta V_{cq} \end{bmatrix} + [B4]_{2*2} \begin{bmatrix} \Delta\omega \\ \Delta V_{cd}^{\#} \end{bmatrix}, \tag{18}$$

$$\begin{bmatrix} \Delta I_{sourd}^{\#} \\ \Delta I_{sourq}^{\#} \end{bmatrix} = [B5]_{2*2} \begin{bmatrix} \Delta V_{cd} \\ \Delta V_{cq} \end{bmatrix} + [B6]_{2*2} \begin{bmatrix} \Delta I_{cd} \\ \Delta I_{cq} \end{bmatrix} + [B7]_{2*2} \begin{bmatrix} \Delta\omega \\ \Delta V_{cd}^{\#} \end{bmatrix}, \tag{19}$$

where

$$[B3]_{2*2} = \begin{bmatrix} sC_{sour} & -\omega^{\#} C_{sour} \\ \omega^{\#} C_{sour} & sC_{sour} \end{bmatrix},$$

$$[B4]_{2*2} = \begin{bmatrix} 0 & 0 \\ V_{cd}^{\#} C_{sour} & 0 \end{bmatrix},$$

$$[B5]_{2*2} = \begin{bmatrix} -G_v^{sour}(s) & -\omega^{\#} C_{sour} \\ \omega^{\#} C_{sour} & -G_v^{sour}(s) \end{bmatrix},$$

$$[B6]_{2*2} = \begin{bmatrix} K & 0 \\ 0 & K \end{bmatrix}, [B7]_{2*2} = \begin{bmatrix} 0 & G_v^{sour}(s) \\ 0 & 0 \end{bmatrix}.$$

The small-signal model of the equations (11)-(16) can be shown as follows:

$$\Delta p_{sour} = 1.5 \begin{pmatrix} V_{cd}\Delta I_{cd} + \Delta V_{cd} I_{cd} \\ +V_{cq}\Delta I_{cq} + \Delta V_{cq} I_{cq} \end{pmatrix}, \tag{20}$$

$$\Delta q_{sour} = 1.5 \begin{pmatrix} V_{cd}\Delta I_{cq} + \Delta V_{cd} I_{cq} \\ -V_{cq}\Delta I_{cd} - \Delta V_{cq} I_{cd} \end{pmatrix}, \tag{21}$$

$$\Delta\omega = -\frac{m\omega_c}{s+\omega_c} \frac{4f-3s}{4f+3s} \Delta p_{sour}, \tag{22}$$

$$\Delta V_{cd}^{\#} = -\frac{n\omega_c}{s+\omega_c} \frac{4f-3s}{4f+3s} \Delta q_{sour}. \tag{23}$$

Similar, the small-signal model of the equations (20)-(23) can be shown as follows:

$$\begin{bmatrix} \Delta\omega \\ \Delta V_{cd}^{\#} \end{bmatrix} = [B8]_{2*2} \begin{bmatrix} \Delta V_{cd} \\ \Delta V_{cq} \end{bmatrix} + [B9]_{2*2} \begin{bmatrix} \Delta I_{cd} \\ \Delta I_{cq} \end{bmatrix}, \tag{24}$$

where

$$[B8]_{2*2} = \begin{bmatrix} \frac{1.5m\omega_c}{s+\omega_c}\frac{4f-3s}{4f+3s} I_{cd}^{\#} & -\frac{1.5m\omega_c}{s+\omega_c}\frac{4f-3s}{4f+3s} I_{cq}^{\#} \\ -\frac{1.5n\omega_c}{s+\omega_c}\frac{4f-3s}{4f+3s} I_{cq}^{\#} & -\frac{1.5n\omega_c}{s+\omega_c}\frac{4f-3s}{4f+3s} I_{cd}^{\#} \end{bmatrix},$$

$$[B9]_{2*2} = \begin{bmatrix} -\frac{1.5m\omega_c}{s+\omega_c}\frac{4f-3s}{4f+3s} V_{cd}^{\#} & 0 \\ 0 & -\frac{1.5n\omega_c}{s+\omega_c}\frac{4f-3s}{4f+3s} V_{cd}^{\#} \end{bmatrix}.$$

Therefore, the output impedance matrix of droop inverter $Z_{inv} = \begin{bmatrix} Z_{dd} & Z_{dq} \\ Z_{qd} & Z_{qq} \end{bmatrix}$ satisfies the following function: $\begin{bmatrix} \Delta V_{cd} \\ \Delta V_{cq} \end{bmatrix} = \begin{bmatrix} Z_{dd} & Z_{dq} \\ Z_{qd} & Z_{qq} \end{bmatrix} \begin{bmatrix} \Delta I_{cd} \\ \Delta I_{cq} \end{bmatrix}$. Thus, apply the equations (18)-(19) and (24) into the equation (17), the output impedance matrix of droop inverter can be obtained, which is shown in the equation (25):

$$\begin{aligned} Z_{inv} &= \begin{bmatrix} Z_{dd} & Z_{dq} \\ Z_{qd} & Z_{qq} \end{bmatrix} \\ &= \begin{Bmatrix} [B5] + [B7][B8] - [B1][B3] \\ -[B1][B4][B8] - [B2][B8] \end{Bmatrix}^{-1} \\ &\quad \begin{Bmatrix} [B1][B4][B9] + [B1] + \\ [B2][B9] - [B6] - [B7][B9] \end{Bmatrix}. \end{aligned} \tag{25}$$

Finally, the load subsystem input admittance matrix can be shown as follows:

$$Y_{load} = {Z_{load}}^{-1} = \begin{bmatrix} Z_{dd} & Z_{dq} \\ Z_{qd} & Z_{qq} \end{bmatrix}^{-1} \tag{26}$$

where R_g, L_g and C_g represents the equivalent circuit impedance. $\omega^{\#}$ represents the rated frequency. Meanwhile,

$Z_{dd} = Z_{qq} = \frac{[Z1]s^2+[Z2]s+[Z3]}{[Z4]s^2+[Z5]s+[Z6]}$,

$Z_{dq} = -Z_{qd} = \frac{[Z7]}{[Z4]s^2+[Z5]s+[Z6]}$,

$[Z1]_{1*1} = \left(L_g C_g + R_g C_g\right) L_g$,

$[Z2]_{1*1} = L_g R_g C_g + R_s^2 C_g + L_g$,

$[Z3]_{1*1} = \left(L_g C_g + R_g C_g\right) L_g \omega^{\#2} + R_g$,

$[Z4]_{1*1} = \left(L_g C_g + R_g C_g\right)^2$,

$[Z5]_{1*1} = 2\left(L_g C_g + R_g C_g\right)$,

$[Z6]_{1*1} = \left(L_g C_g + R_g C_g\right)^2 \omega^{\#2} + 1$,

$[Z7]_{1*1} = \left(L_g C_g + R_g C_g\right) R_g \omega^{\#} - L_g \omega^{\#}$.

Thus, the return-ratio matrix is shown as follows:

$$R_0 = Z_{sour} Y_{load}. \tag{27}$$

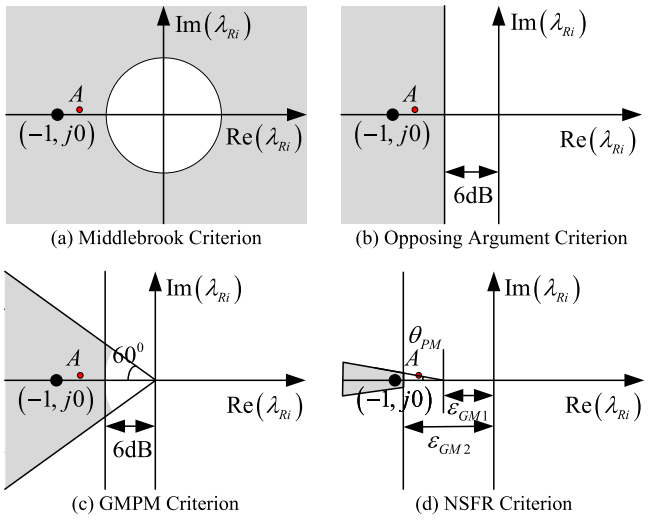

(a) Middlebrook Criterion (b) Opposing Argument Criterion

(c) GMPM Criterion (d) NSFR Criterion

Fig. 5. Stability forbidden criterion.

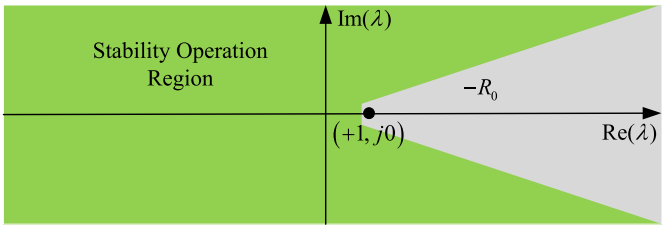

Fig. 6. Stability operation region.

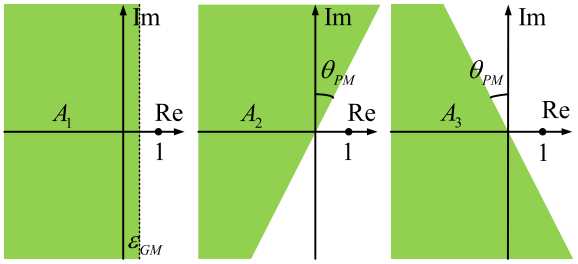

Fig. 7. Set of stability operation regions.

Noting that the return-ratio matrix R_0 is the delay-dependent function, i.e., $R_0 = f(T)$. According to the impedance-based approach [25], the system is stable if and only if the generalized Nyquist curve of the return-ratio matrix R_0 does not contain $(-1, j0)$ points.

III. Adaptive Step Search Approach

In this section, the minimum switching/sampling frequency regarding grid-connected inverters with the digital control system under weak grid is provided. Due to the complex Nyquist curve drawing precess, numerous simplified stability forbidden region criteria have been proposed, which is shown in Fig. 5 [21]. Compared with Middlebrook criterion, Opposing Argument criterion and GMPM criterion, NSFR criterion proposed in our previous literature [21] has lower conservatism. Noting that the approximate necessary and sufficient condition can be obtained if ε_{GM} tends to one and θ_{PM} tends to 90^0, where ε_{GM} and θ_{PM} represents gain and phase margins. Based on this, NSFR criterion is applied to analyze stability regarding the delay-dependent return ratio matrix.

Lemma 1: [21] The system is stable if and only if the generalized Nyquist curve of the negative return-ratio matrix $(-R_0)$ does not contain $(1, j0)$ points.

Thus, the stability operation region can be obtained through $-R_0$, which is green region in Fig. 6. Furthermore, the stability operation region can be provided through the union of three subregions (green region in Fig. 7), i.e., $A = A_1 \cup A_2 \cup A_3$. A_1 can transform the original matrix into the space plane formed by Hurwitz matrix (R_1) by translation mapping, A_2 and A_3 can transform the original matrix into Hurwitz matrix (R_2 and R_3) by transformation mapping respectively, and then, R_1, R_2 and R_3 can be defined as generalized return-ratio matrix, which are shown as follows:

$$A_1: \quad R_1 = -R_0 - \varepsilon_{GM} E. \tag{28}$$

$$A_2: \quad R_2 = -R_0 \times e^{j\theta_{PM}}. \tag{29}$$

$$A_3: \quad R_3 = -R_0 \times e^{-j\theta_{PM}}. \tag{30}$$

where R_1, R_2 and R_3 are Hurwitz. To sum up, the system is stable if one of the generalized return-ratio matrices is Hurwitz.

Remark 1: Based on the novel stability forbidden/operation region criterion proposed in our previous literature [23], the switching/sampling frequency threshold identification regarding grid-connected inverters with the digital control system is switched into the identification problem whether the generalized return-ratio matrix is one Hurwitz matrix. Traditionally, the point-point simulation approach is also able to provide the minimum switching/sampling frequency value. However, thousands of Nyquist curve drawing process should be executed through power simulation engineers. Especially when the number of the grid-connected inverters is large, the point-point simulation approach is not suitable. Through the proposed criterion and proposed adaptive step search approach in this paper, thousands of Nyquist curve drawing process can be eliminated, which reduces the computational burden a lot.

Through the foresaid analysis, if one of the R_1, R_2 and R_3 is Hurwitz, the system is stable. To this end, the generalized return-ratio matrix is one sampling/switching frequency dependent nonlinear time invariant matrix. Therefore, this paper proposes an adaptive step search approach to obtain the stability-oriented minimum sampling/switching frequency. In order to extend the adaptability of the algorithm, this paper uses the least mean square (LMS) as the growth factor, which is shown as follows:

$$r(m+1) = sign(L_{\min}) \times \Delta r(0) \times |L_{\min}|^{\lambda(m)} + r(m), \tag{31}$$

$$\lambda(m) = \alpha \times \left(1 + e^{-\beta |s(m)|^2}\right), \tag{32}$$

$$s(m) = \gamma\, s(m-1) + (1-\gamma)\, L_{\min}, \tag{33}$$

where $sign(x)$ represents sign function. L_{min} represents the real part of the minimum eigenvalue of the generalized return-ratio matrix. $|L_{\min}|^{\lambda(m)}$ and $\lambda(m)$ represents variable step

Algorithm 1 *Solving Process*

Initialization: $r(0) = 0$; $m = 0$ and $\Delta r(0) = 0$.

Iteration: $(i \leq p)$

1: Initialization $L_{max1} = \emptyset$, $L_{max2} = \emptyset$, $L_{max3} = \emptyset$ and $i = 1$;

2: Compute the generalized return-ratio matrix $R(s)$ under $s = -j2\pi f_i$, i.e., R_1, R_2 and R_3;

3: Compute the maximum real part of three generalized return-ratio matrices, i.e., $L_1 = max(real(eig(R_1)))$, $L_2 = max(real(eig(R_2)))$ and $L_3 = max(real(eig(R_3)))$;

4: Extend matrix $L_{max1} = [L_{max1}, L_1]$, $L_{max2} = [L_{max2}, L_2]$ and $L_{max3} = [L_{max3}, L_3]$. If $i < 20000$, $i = i + 1$, turn to 2. Else, turn to 5;

5: Select the maximum value among L_{max1}, L_{max2} and L_{max3}, i.e., $L_{max-1} = max(L_{max1})$, $L_{max-2} = max(L_{max2})$ and $L_{max-3} = max(L_{max3})$. Define L_{min} is the minimum value among L_{max-2}, L_{max-1} and L_{max-3}, i.e., $L_{min} = min(L_{max-2}, L_{max-1}, L_{max-3})$;

6: Judge whether $r(m)$ is equal to zero under L_{min}. If yes, the records of the open interval $(0, r(m))$ are stored, and then 7 is entered. If not, turn to 1;

7: Compute the set of all open sets in 6, and record the result as the maximum value of equivalent delay time T_{min}.

factor and step growth factor. α and β represents adjustment factor, and γ represents forgetting factor. The detailed solving process can be shown in **Algorithm 1**:

Through **Algorithm 1**, the minimum switching/sampling frequency regarding grid-connected inverters with the digital control system under weak grid is provided as $f_{\min} = 1/T_{\max}$.

Remark 2: The proposed adaptive step search approach regarding minimum switching/sampling frequency belongs to the variation of dichotomy, and the relationship between L_{min} and $r(m)$ is shown in Fig. 8, which has monotonic increasing characteristic [12]. Therefore, the convergence of the proposed approach is ensured, and it is not affected through the selection of initial value. This modified dichotomy approach has been widely applied to power system, i.e., the disturbance observation method for maximum power point tracking and the initial value selection method for power flow calculation [27]. In this paper, the adaptability of the proposed algorithm focuses more on convergence speed, which ensures that this method is suitable for systems requiring fast calculation time. The traditional fixed step search method has one slow convergence. Thus, this paper applies the characteristics of exponential function, which has the characteristics of low change rate at the convergence point (0 value) and high change rate far away from the convergence point. In other words, this method can make sure to search in small steps near the convergence point and in large steps away from the convergence point [27]. By setting the least mean square as the exponential term and using the properties of the exponential function, the convergence speed of the algorithm is improved, so as to improve the applicability of the algorithm and solve the high computing speed requirements.

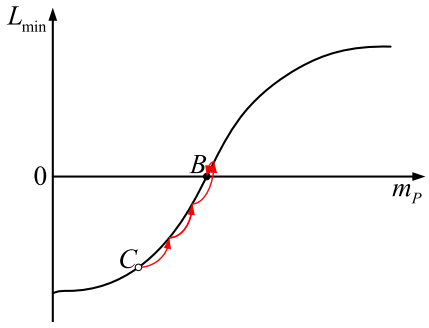

Fig. 8. Relationship curve between L_{min} and T_{max}.

TABLE I

THE SIMULATION/EXPERIMENTAL SYSTEM PARAMETERS

Parameters	Values	Parameters	Values
Voltage controller	$G_v^{sour} = 1 + 8/s$	DC bus voltage	$700V$
Current controller	$G_c^{sour} = 4 + 150/s$	Rated voltage	$220V$
Filter capacitor	$600\mu F$	Rated frequency	$50Hz$
Filter inductor	$6mH$	Cut-off frequency	$5Hz$

Remark 3: In this paper, the upper limit of i in the algorithm is 20000. In other words, system frequency should be verified from 0Hz to 20000Hz under the minimum switching frequency regarding IGBT. The reason that the upper limit of i is set as 20000 is that the motivation of this paper is to explore conditions of broadband oscillation phenomena such as low frequency and sub/super-synchronous oscillation caused by the decrease of switching frequency. Traditionally, the interval regarding broadband oscillation is about [0, 3000]Hz. In order to ensure the effectiveness of this method under extreme conditions, this paper improves the verification frequency range. If engineers want to calculate the results quickly, the upper limit i can be reduced to 3000.

IV. SIMULATION RESULTS

In order to verify the high performance of the proposed minimum switching/sampling frequency identification based on adaptive step search approach for grid-connected inverters with the digital control system under weak grid, the simulation test system provided in the literature [25] is provided. The relative control parameters are shown in Table I, and the number of the grid-connected inverters is set as three. Meanwhile, the line impedance of the weak grid is shown as follows: $R_g = 0.25\Omega$. $L_g = 10mH$ and $C_g = 100\mu F$. Based on the proposed adaptive step search approach regarding the generalized return-ratio matrix, the minimum switching/sampling frequency is 3.662kHz. In this paper, the stability of the grid-connected inverters with the digital control system under different switching/sampling frequencies will be provided, respectively, The effectiveness of the proposed adaptive step search algorithm based on generalized return-ratio matrix will be verified by simulating the waveform of AC bus voltage of the grid-connected inverters with the digital control system in MATLAB/Simulink, which are shown as follows:

Firstly, the switching/sampling frequency of the grid-connected inverters with the digital control system is 4kHz,

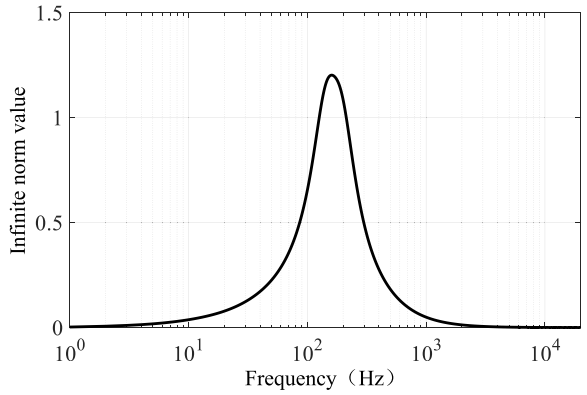

Fig. 9. Infinite norm criterion.

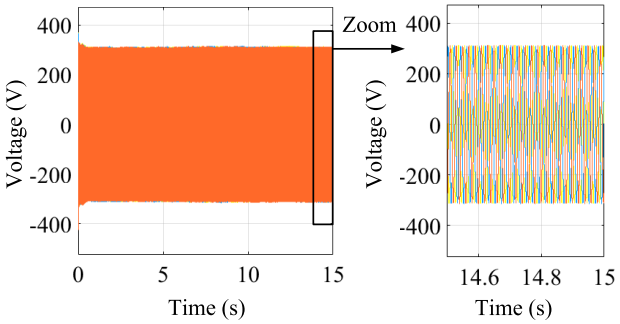

Fig. 10. Voltage waveform under 4kHz of IGBT.

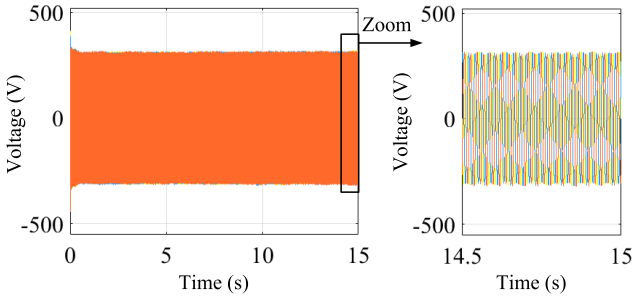

Fig. 11. Voltage waveform under 3.5kHz of IGBT.

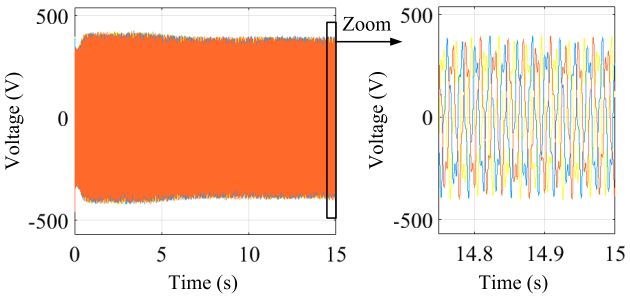

Fig. 12. Voltage waveform under 3kHz of IGBT.

which is obviously higher than the minimum switching/sampling frequency obtained by the proposed identification approach. To this end, the system can remain stable. As shown in Fig. 9, which is based on the literature [22], the infinite norm regarding the return ratio matrix of the system is bigger than unit in the frequency interval [126Hz, 212Hz]. Based on this, it is possible that the system is unstable. The actual voltage waveform of the grid-connected inverters with the digital control system is shown in Fig. 10, and the system maintains stability. To sum up, compared with the existing literature [22], this method has lower conservatism. Meanwhile, the high performance of the proposed minimum switching/sampling frequency identification approach can be ensured.

Secondly, the switching/sampling frequency of the grid-connected inverters with the digital control system is reset as 3.5kHz, which is slightly less than the minimum switching/sampling frequency obtained by the proposed identification approach. Under this case, it is possible that the simulation system is not stable. The actual voltage waveform of the grid-connected inverters with the digital control system is shown in Fig. 10, and the system has low frequency oscillation. The simulation results illustrate that the high performance of the proposed minimum switching/sampling frequency identification approach can be ensured.

Thirdly, the switching/sampling frequency of the grid-connected inverters with the digital control system is reset as 3kHz, which is less than the minimum switching/sampling frequency obtained by the proposed identification approach. According to the proposed criterion, the system cannot remain stable. The actual voltage waveform of the grid-connected inverters with the digital control system is shown in Fig. 11, and the system has a large low-frequency oscillation and sub-synchronous oscillation. As a result, the simulation results show that the high performance of the proposed minimum switching/sampling frequency identification approach can be verified.

Fourthly, the switching/sampling frequency of the grid-connected inverters with the digital control system is reset as 2kHz, which is obviously less than the minimum switching/sampling frequency obtained by the proposed identification approach a lot. Under this frequency, the system cannot remain stable. The actual voltage waveform of the grid-connected inverters with the digital control system is shown in Fig. 12, and the system has a large divergent oscillation. If no effective suppression measures are taken, the system will induce extreme phenomena such as over-current/over-voltage protection and disconnection. Under this case, the devices in micro-grid are easily damaged. Consequently, the simulation results illustrate that the high performance of the proposed minimum switching/sampling frequency identification approach can be well verified.

Through the foresaid simulation results under different frequencies, the effectiveness regarding the proposed minimum switching/sampling frequency identification based on adaptive step search approach for grid-connected inverters with the digital control system under weak grid can be fully proved.

V. Experimental Results

In order to verify the high performance of the proposed minimum switching/sampling frequency identification based on adaptive step search approach for grid-connected inverters

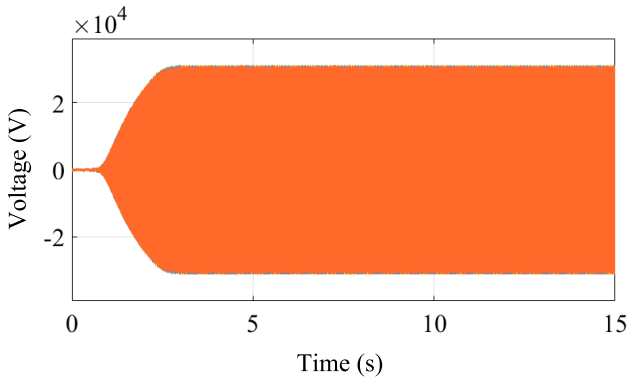

Fig. 13. Voltage waveform under 2kHz of IGBT.

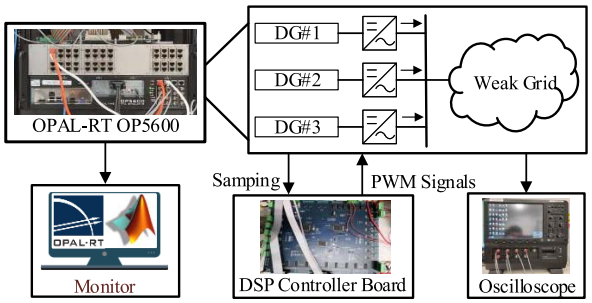

Fig. 14. Hardware-in-the-loop test system diagram.

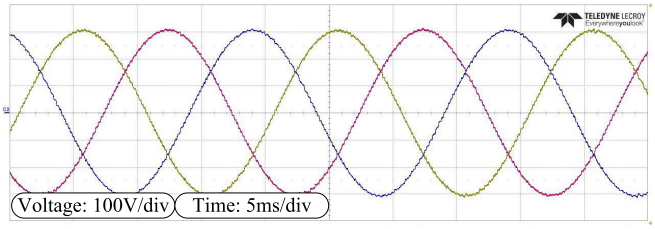

Fig. 15. Experimental voltage waveform under 4kHz of IGBT.

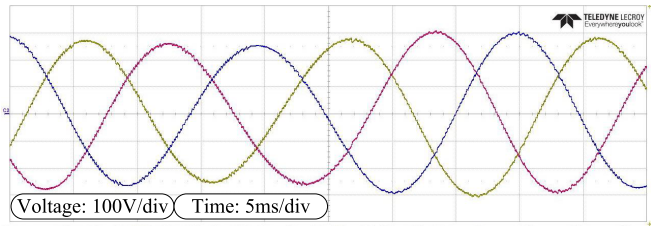

Fig. 16. Experimental voltage waveform under 3.5kHz of IGBT.

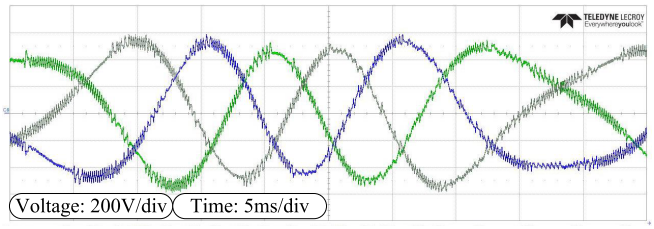

Fig. 17. Experimental voltage waveform under 3kHz of IGBT.

with the digital control system under weak grid, the controller hardware-in-the-loop (CHIL) experiments are executed in OPAL-RT real-time simulation system with the system parameters are the same as the simulation section. The CHIL experiment facility is cited in our previous literature [26]. The detailed experimental figure is shown in Fig. 13. Therein, the relative control parameters are also shown in Table I, and the number of the grid-connected inverters is set as three. Meanwhile, the line impedance of the weak grid is also shown as follows: $R_g = 0.25\Omega$. $L_g = 10mH$ and $C_g = 100\mu F$. Based on the proposed adaptive step search approach regarding the generalized return-ratio matrix, the minimum switching/sampling frequency is also 3.662kHz. The effectiveness of the proposed adaptive step search algorithm based on generalized return-ratio matrix will be verified by the experimental waveform of AC bus voltage of the grid-connected inverters with the digital control system in CHIL experiments, which are expressed below:

Firstly, the switching/sampling frequency of the grid-connected inverters with the digital control system is set as 4kHz, which is obviously higher than the minimum switching/sampling frequency obtained by the proposed identification approach. Under this frequency, the system should remain stable. The actual experimental voltage waveform of the grid-connected inverters with the digital control system is shown in Fig. 14, and the experimental system maintains stability. Based on this, the high performance of the proposed minimum switching/sampling frequency identification approach can be ensured through experiment results.

Secondly, the switching/sampling frequency of the grid-connected inverters with the digital control system is reset as 3.5kHz, which is slightly less than the minimum switching/sampling frequency obtained by the proposed identification approach. Under this case, it is possible that the experimental system is not stable. The actual experimental voltage waveform of the grid-connected inverters with the digital control system is shown in Fig. 15, and the experimental system has low frequency oscillation. The experimental results illustrate that the high performance of the proposed minimum switching/sampling frequency identification approach can be ensured.

Thirdly, the switching/sampling frequency of the grid-connected inverters with the digital control system is reset as 3kHz, which is less than the minimum switching/sampling frequency obtained by the proposed identification approach. According to the proposed criterion, the experimental system cannot remain stable. The actual experimental voltage waveform of the grid-connected inverters with the digital control system is shown in Fig. 16, and the system has a large low-frequency oscillation and sub-synchronous oscillation. As a result. If no effective suppression measures are taken, the relative device may be damaged. Consequently, the simulation results illustrate that the high performance of the proposed minimum switching/sampling frequency identification approach can be well verified.

The simulation results were validated through experimental results, which illustrates that the proposed minimum switching/sampling frequency identification approach based on adaptive step search approach for grid-connected inverters with the digital control system under weak grid has high effectiveness.

VI. Conclusion

Grid-connected inverters with the digital control system have been regarded as one simplest and typical cyber-physical system. Meanwhile, the switching/sampling frequency of the inverter has been always selected as low as possible from an efficiency viewpoint, resulting in unavoidable delay time. Therein, this delay time has been prone to the system instability, which is more prone to severity under weak grid. Traditionally, almost scholars have focused more on system stability with communication time delay or attack. To this end, this paper has proposed a minimum switching/sampling frequency identification approach based on adaptive step search approach for grid-connected inverters under weak grid. Compared with the existing literatures, three advantages have been found in this paper as follows:

(1) In order to reflect the cyber-physical interaction impact, the equivalent delay time has been constructed through the system impedance model. Based on this, the cyber-physical interaction impact problem can be transformed into the switching/sampling frequency threshold identification problem;

(2) Based on the novel stability forbidden/operation region criterion, the switching/sampling frequency threshold identification has been switched into the Hurwitz matrix identification problem, which reduces the computational burden;

(3) In order to obtain the minimum switching/sampling frequency, an adaptive step search approach with low conservatism has been proposed. Meanwhile, the convergence of the proposed approach has been verified, which is independent for the initial condition.

Finally, the simulation and experimental results have been provided to illustrate that the proposed minimum switching/sampling frequency identification approach based on adaptive step search approach for grid-connected inverters with the digital control system under weak grid is highly effective. Therein, the method in this paper can well evaluate the system stability under different frequencies through simulation and experiment.

In the future, the whole stability analysis consisting the primary controller, secondary controller and third controller, should be studied to promote the development of system stability regarding cyber-physical systems.

References

[1] *Cyber-Physical Systems. Program Announcements & Information*, Nat. Sci. Found., Arlington, VA, USA, Sep. 2008.

[2] Y. Yang, D. Xu, T. Ma, and X. Su, "Adaptive cooperative terminal sliding mode control for distributed energy storage systems," *IEEE Trans. Circuits Syst. I, Reg. Papers*, vol. 68, no. 1, pp. 434–443, Jan. 2021.

[3] Y. Huang and J. Zhao, "Cyber-physical systems with multiple denial-of-service attackers: A game-theoretic framework," *IEEE Trans. Circuits Syst. I, Reg. Papers*, early access, Jul. 27, 2021, doi: 10.1109/TCSI.2021.3098335.

[4] C. Dong, Q. Xiao, M. Wang, T. Morstyn, M. D. McCulloch, and H. Jia, "Distorted stability space and instability triggering mechanism of EV aggregation delays in the secondary frequency regulation of electrical grid-electric vehicle system," *IEEE Trans. Smart Grid*, vol. 11, no. 6, pp. 5084–5098, Nov. 2020.

[5] R. Wang, Q. Sun, D. Ma, and Z. Liu, "The small-signal stability analysis of the droop-controlled converter in electromagnetic timescale," *IEEE Trans. Sustain. Energy*, vol. 10, no. 3, pp. 1459–1469, Jul. 2019.

[6] X. He, R. Wang, J. Wu, and W. Li, "Nature of power electronics and integration of power conversion with communication for talkative power," *Nature Commun.*, vol. 11, no. 1, pp. 2479–2490, May 2020.

[7] X. Hu, H. Wang, and X. Tang, "Cyber-physical control for energy-saving vehicle following with connectivity," *IEEE Trans. Ind. Electron.*, vol. 64, no. 11, pp. 8578–8587, Nov. 2017.

[8] D. Lv, A. Eslami, and S. Cui, "Load-dependent cascading failures in finite-size Erdös-Rényi random networks," *IEEE Trans. Netw. Sci. Eng.*, vol. 4, no. 2, pp. 129–139, Apr./Jun. 2017.

[9] Y. Wan, J. Cao, G. Chen, and W. Huang, "Distributed observer-based cyber-security control of complex dynamical networks," *IEEE Trans. Circuits Syst. I, Reg. Papers*, vol. 64, no. 11, pp. 2966–2975, Nov. 2017.

[10] L. Xu, Q. Guo, Z. Wang, and H. Sun, "Modeling of time-delayed distributed cyber-physical power systems for small-signal stability analysis," *IEEE Trans. Smart Grid*, vol. 12, no. 4, pp. 3425–3437, Jul. 2021, doi: 10.1109/TSG.2021.3052303.

[11] C. Dong *et al.*, "Time-delay stability analysis for hybrid energy storage system with hierarchical control in DC microgrids," *IEEE Trans. Smart Grid*, vol. 9, no. 6, pp. 6633–6645, Nov. 2018.

[12] R. Wang, Q. Sun, P. Zhang, Y. Gui, and P. Wang, "Reduced-order transfer function model of the droop-controlled inverter via Jordan continued-fraction expansion," *IEEE Trans. Energy Convers.*, vol. 35, no. 3, pp. 1585–1595, Sep. 2020.

[13] Y. Xu, H. Nian, and L. Chen, "Small-signal modeling and analysis of DC-link dynamics in type-IV wind turbine system," *IEEE Trans. Ind. Electron.*, vol. 68, no. 2, pp. 1423–1433, Feb. 2021.

[14] E. A. A. Coelho, P. C. Cortizo, and P. F. D. Garcia, "Small-signal stability for parallel-connected inverters in stand-alone AC supply systems," *IEEE Trans. Ind. Appl.*, vol. 38, no. 2, pp. 533–542, Mar./Apr. 2002.

[15] N. Pogaku, M. Prodanovic, and T. C. Green, "Modeling, analysis and testing of autonomous operation of an inverter-based microgrid," *IEEE Trans. Power Electron.*, vol. 22, no. 2, pp. 613–625, Mar. 2007.

[16] R. Wang, Q. Sun, P. Tu, J. Xiao, Y. Gui, and P. Wang, "Reduced-order aggregate model for large-scale converters with inhomogeneous initial conditions in DC microgrids," *IEEE Trans. Energy Convers.*, vol. 36, no. 3, pp. 2473–2484, Sep. 2021, doi: 10.1109/TEC.2021.3050434.

[17] H. Hu, P. Pan, Y. Song, and Z. He, "A novel controlled frequency band impedance measurement approach for single-phase railway traction power system," *IEEE Trans. Ind. Electron.*, vol. 67, no. 1, pp. 244–253, Jan. 2020.

[18] J. Sun, "Impedance-based stability criterion for grid-connected inverters," *IEEE Trans. Power Electron.*, vol. 26, no. 11, pp. 3075–3078, Nov. 2011.

[19] R. D. Middlebrook, "Input filter considerations in design and application of switching regulators," in *Proc. IEEE Ind. Appl. Soc. Annu. Meeting*, Oct. 1976, pp. 366–382.

[20] J. M. Undrill and T. E. Kostyniak, "Subsynchronous oscillations Part 1 comprehensive system stability analysis," *IEEE Trans. Power App. Syst.*, vol. PAS-95, no. 4, pp. 1446–1455, Jul. 1976.

[21] W. Rui, S. Qiuye, M. Dazhong, and H. Xuguang, "Line impedance cooperative stability region identification method for grid-tied inverters under weak grids," *IEEE Trans. Smart Grid*, vol. 11, no. 4, pp. 2856–2866, Jul. 2020.

[22] Z. Liu, J. Liu, W. Bao, and Y. Zhao, "Infinity-norm of impedance-based stability criterion for three-phase AC distributed power systems with constant power loads," *IEEE Trans. Power Electron.*, vol. 30, no. 6, pp. 3030–3043, Jun. 2015.

[23] A. Riccobono and E. Santi, "Comprehensive review of stability criteria for DC power distribution systems," *IEEE Trans. Ind. Appl.*, vol. 50, no. 5, pp. 3525–3535, Sep./Oct. 2014.

[24] S. D. Sudhoff, S. F. Glover, P. T. Lamm, D. H. Schmucker, and D. E. Delisle, "Admittance space stability analysis of power electronic systems," *IEEE Trans. Aerosp. Electron. Syst.*, vol. 36, no. 3, pp. 965–973, Jul. 2000.

[25] R. Wang, Q. Sun, W. Hu, J. Xiao, H. Zhang, and P. Wang, "Stability-oriented droop coefficients region identification for inverters within weak grid: An impedance-based approach," *IEEE Trans. Syst., Man, Cybern., Syst.*, vol. 51, no. 4, pp. 2258–2268, Apr. 2021.

[26] C. Dong, S. Yang, H. Jia, and P. Wang, "Padé-based stability analysis for a modular multilevel converter considering the time delay in the digital control system," *IEEE Trans. Ind. Electron.*, vol. 66, no. 7, pp. 5242–5253, Jul. 2019.
[27] Q. Sun, Q. Dong, S. You, Z. Li, and R. Wang, "A unified energy flow analysis considering initial guesses in complex multi-energy carrier systems," *Energy*, vol. 213, Dec. 2020, Art. no. 118812.
[28] Z. Zhang *et al.*, "A modulized three-port interlinking converter for hybrid AC/DC/DS microgrids featured with a decentralized power management strategy," *IEEE Trans. Ind. Electron.*, vol. 68, no. 12, pp. 12430–12440, Dec. 2021, doi: 10.1109/TIE.2020.3040660.

Rui Wang (Student Member, IEEE) received the B.S. degree in electrical engineering and automation and the Ph.D. degree in power electronics and power drive from Northeastern University, Shenyang, China, in 2016 and 2021, respectively. He is currently a Lecturer with Northeastern University. He has authored or coauthored over 50 articles, and authorized over 20 invention patents. His research interest includes cooperative control of distributed generation and its stability analysis of electromagnetic timescale in cyber-energy systems.

Qiuye Sun (Senior Member, IEEE) received the Ph.D. degree in control science and engineering from Northeastern University, Liaoning, China, in 2007. He is currently a Full Professor with Northeastern University. He has authored or coauthored over 200 articles, authorized over 100 invention patents, and published over ten books or textbooks. His current research interests include optimization analysis technology of power distribution networks, network control of energy internet, integrated energy systems, and microgrids. He is an IET Fellow. He is an Associate Editor of IEEE TRANSACTIONS ON NEURAL NETWORKS AND LEARNING SYSTEMS, *IET Cyber-Physical Systems*, *CSEE Journal of Power and Energy Systems*, IEEE/CAA JOURNAL OF AUTOMATICA SINICA, and *International Transactions on Electrical Energy Systems*.

Huaguang Zhang (Fellow, IEEE) received the B.S. and M.S. degrees in control engineering from Northeast Dianli University, Jilin, China, in 1982 and 1985, respectively, and the Ph.D. degree in thermal power engineering and automation from Southeast University, Nanjing, China, in 1991.

He joined the Department of Automatic Control, Northeastern University, Shenyang, China, as a Post-Doctoral Fellow, in 1992, for a period of two years. Since 1994, he has been a Professor and the Head of the School of Information Science and Engineering, Institute of Electric Automation, Northeastern University. He has authored and coauthored over 280 journal articles and conference papers, six monographs, and co-invented 90 patents. His main research interests include fuzzy control, stochastic system control, neural networks-based control, nonlinear control, and their applications. He was awarded the Outstanding Youth Science Foundation Award from the National Natural Science Foundation Committee of China in 2003. He was named the Cheung Kong Scholar by the Education Ministry of China in 2005. He was a recipient of the IEEE TRANSACTIONS ON NEURAL NETWORKS 2012 Outstanding Paper Award. He is the E-Letter Chair of the IEEE CIS Society and the Former Chair of the Adaptive Dynamic Programming and Reinforcement Learning Technical Committee on IEEE Computational Intelligence Society. He is an Associate Editor of *Automatica*, IEEE TRANSACTIONS ON NEURAL NETWORKS, IEEE TRANSACTIONS ON CYBERNETICS, and *Neurocomputing*. From 2008 to 2013, he was an Associate Editor of IEEE TRANSACTIONS ON FUZZY SYSTEMS.

Lei Liu (Senior Member, IEEE) received the B.S. degree in information and computing science and the M.S. degree in applied mathematics from Liaoning University of Technology, Jinzhou, China, in 2010 and 2013, respectively, and the Ph.D. degree in control theory and control engineering from Northeastern University, Shenyang, China, in 2017. He is currently an Associate Professor with the College of Science, Liaoning University of Technology. His current research interests include fault-tolerant control, fault detection and diagnosis, optimal control for nonlinear systems, and neural network control and their industrial applications.

Yonghao Gui (Senior Member, IEEE) received the B.S. degree in automation from Northeastern University, Shenyang, China, in 2009, and the M.S. and Ph.D. degrees in electrical engineering from Hanyang University, Seoul, South Korea, in 2012 and 2017, respectively.

From February 2017 to November 2018, he worked as a Post-Doctoral Researcher with the Department of Energy Technology, Aalborg University, Aalborg, Denmark. Since December 2018, he has been working with the Automation and Control Section, Department of Electronic Systems, Aalborg University, where he is currently an Assistant Professor. His research interests include control of power electronics in power systems, energy internet, and smart grids. He was a recipient of the IEEE Power & Energy Society General Meeting Best Conference Paper Award in 2019 and the IJCAS Academic Activity Award 2019. He has served as an Associate Editor for the IEEE TRANSACTION ON ENERGY CONVERSION, IEEE ACCESS, and *International Journal of Control, Automation and Systems* (IJCAS).

Peng Wang received the B.Sc. degree in electronic engineering from Xi'an Jiaotong University, Xi'an, China, in 1978, the M.Sc. degree from Taiyuan University of Technology, Taiyuan, China, in 1987, and the M.Sc. and Ph.D. degrees in electrical engineering from the University of Saskatchewan, Saskatoon, SK, Canada, in 1995 and 1998, respectively. He is currently a Full Professor with the School of Electrical and Electronic Engineering, Nanyang Technological University, Singapore. His current research interests include power system planning and operation, renewable energy planning, solar/electricity conversion systems, and power system reliability analysis. He is an Associate Editor or a Guest Editor-in-Chief of IEEE TRANSACTIONS ON SMART GRID, IEEE TRANSACTIONS ON POWER DELIVERY, *Journal of Modern Power Systems and Clean Energy*, and *CSEE Journal of Power and Energy Systems*.